PHYSICAL REVIEW B **80**, 161304(R) (2009)

# Terahertz radiation in semiconductor quantum dots driven by gigahertz waves: The role of tailoring the quasienergy spectrum

Suqing Duan, Wei Zhang,* Yan Xie, Weidong Chu, and Xian-geng Zhao
*Institute of Applied Physics and Computational Mathematics, P.O. Box 8009(28), Beijing 100088, China*
(Received 3 September 2009; published 14 October 2009)

We explore the terahertz (THz) radiation from high-order harmonic fields in semiconductor quantum dots driven by gigahertz (GHz) waves, due to the availability of high power GHz sources. By mapping the optical problem to a transport problem, we are able to uncover several features in the THz wave generation processes. With the help of the Floquet theorem, the efficiency of THz wave generation, which is related to the particle transport, is determined by the bandwidth of the quasienergy spectrum. We not only reveal the interesting relation between optical processes and transport phenomena, but also find the optimal conditions (corresponding to resonances) and quench conditions (corresponding to band collapses) for THz wave generation. The nice on/off properties (the ratio of emission intensity at resonance to that at quench condition $\sim 10^6$) are helpful for the design of THz source and have important applications in nanodevices with THz wave involved.

DOI: 10.1103/PhysRevB.80.161304 PACS number(s): 78.67.Hc, 42.50.Ct, 42.65.Ky

## I. INTRODUCTION

Terahertz (THz) wave is the electromagnetic wave with frequency between 0.1–10 THz. It has drastic applications in biosensor, medical image, security, astronomy, environmental monitoring, etc.,[1] partially because the frequencies in this regime match the oscillation spectra of many molecules. Despite its extensive-application driving development, THz still remains the least developed spectral regime. One of the key problems is the THz wave generation, which forms the basis for its further studies and applications. The THz gap is between those generated by classical circuits and those generated by quantum transitions. The lack of nature objects with suitable energy spectrum makes the THz wave generation a challenge problem.

Several proposals for THz radiation generation have been proposed and some of them have been realized in experiments. These approaches are either based on solid-state electronic devices (transistor, Gunn oscillators, and Schottky diode multipliers) or by optical generation through nonlinear effect,[2] or direct generation, such as free-electron laser.[3] One breakthrough is the quantum cascade laser (QCL) based on semiconductor superlattices.[4] Recently Ahn *et al.* suggested an interesting approach based on semiconductor nanostructures driven by acoustic wave,[5] and Chassagneux *et al.* developed electrically pumped photonic-crystal THz lasers.[6] These approaches have their own advantages and disadvantages. In general it is difficult to build a THz wave generator with high quality, i.e., in a compact form, with high power, working at suitable temperature. Much more efforts in this direction are needed.

Because of the lack of appropriate materials with suitable band gaps, the THz wave can either be generated from waves in optical regimes by nonlinear effects (such as difference frequency method), or by multiplication from millimeter-wave [gigahertz (GHz)] regime. In this Rapid Communication, we adopt the second approach to investigate the THz wave generation, since it is much easier to obtain the high power radiation of low frequency. For instance, the power of radiation with frequency around 10–100 GHz generated by impact ionization avalanche transition-time (IMPATT) diode can be as high as 1 W. We tackle this issue by mapping the current optical problem to a transport problem, which has been explored a lot.[7] We find that the efficiency of THz wave generation is determined by the quasienergy spectrum, which usually plays an essential role in charge transport driven by an AC electric field. With the help of the Floquet theorem,[8] we find the optimal conditions (corresponding to resonances) and the quench conditions (corresponding to band collapses/coherent destruction of tunneling)[9–11] for THz wave generation from the analysis of quasienergy spectrum. Our studies can give guidance for the design of THz sources and related devices.

## II. THEORETICAL FORMALISM

Our system consists of a quantum dot (QD) with states $|1\rangle$, $|2\rangle$ driven by a low frequency ($\omega_0$ in the GHz regime) field, which can be generated by other methods such as IMPATT diode, or even phonon field.[5] Usually, the energy spacing between the two states in the QD $\Delta = E_2 - E_1$ is much larger than $\hbar\omega_0$. The THz emission is obtained as the high-order harmonic response of QD to the driving field. The system and related optical processes illustrated schematically in Fig. 1(a) can be described by the Hamiltonian[5]

$$H = H_0 + H_{pt} + H_{e-pt} + H_{e-em}, \tag{1}$$

with $H_0 = \Sigma_{i=1,2} E_i a_i^+ a_i$, $H_{pt} = \Sigma_q \hbar\nu_q c_q^+ c_q$, $H_{e-pt} = \Sigma_q g(q) a_i^+ a_j (c_q - c_q^+)$, and $H_{e-em} = G \sin(\omega_0 t) a_i^+ a_j$, where $a_i$ is the annihilation operator for electron, $c_q$ the annihilation operator for photon, $g_q = (\hbar\nu_q / 2\varepsilon_0 V)^{1/2}$ the electron-photon coupling constant (we have neglected the polarization dependence for simplicity). The driving field is described by a classical field $G \sin(\omega_0 t)$ since it's frequency is low and the field strength is usually very large. The emission spectrum $S(\omega)$ can be calculated as $S(\omega) = n_q(t)/tg_q^2$, where $n_q = \langle c_q^+ c_q \rangle$ is the photon number operator for mode $q$. We will call the basic excitation of driving field as $D$-photon and that of the emission field as $E$-photon in this Rapid Communication for convenience. We present a set of basis $|i, n_i\rangle$, $i = 1, 2$, for states with electron in state $|i\rangle$ and $n_i$ photons. The above model can be mapped to another model of particle transport

 

in a two-chain system. The states $|1,m\rangle$ ($|2,m\rangle$) are mapped to the states of the particle at site m on chain I (II). The effective Hamiltonian can be written as

$$H_{eff} = \sum_m (E_1 + m\hbar\nu_q)a_m^+ a_m + \sum_m (E_2 + m\hbar\nu_q)b_m^+ b_m + g_q\sqrt{m}(a_m^+ b_{m-1} + b_m^+ a_{m-1}) + G\sin(\omega_0 t)(a_m^+ b_m + b_m^+ a_m), \quad (2)$$

where $a_m$ ($b_m$) are the annihilation operators for states $|1,m\rangle$ ($|2,m\rangle$). To make further steps in analytical analysis, we use an effective $g$ to replace $g_q\sqrt{m}$. This approximation may be OK for small $g_q$ and the validity of this approximation is justified by exact numerical calculations based on Eq. (1).

With the help of transformation $\alpha_k = \Sigma_{m\geq 0} e^{-imk-im\omega_0 t}a_m$ and $\beta_k = \Sigma_{m\geq 0} e^{-imk-im\omega_0 t}b_m$, the Schrodinger equation can be written in the form

$$i\begin{pmatrix} \frac{d\alpha}{dt} \\ \frac{d\beta}{dt} \end{pmatrix} = \left[\frac{\Delta}{2}\sigma_z + \phi(k,t)\sigma_x\right]\begin{pmatrix}\alpha \\ \beta\end{pmatrix}, \quad (3)$$

where $\phi(k,t) = g\cos(k+\nu t) + G\sin(\omega_0 t)$, $\sigma_z$, $\sigma_x$ the Pauli matrices, and we have set $\hbar = 1$. A formal solution was obtained for Eq. (3) in Ref. 12. The evolution operator for Eq. (3) can be written in a compact form $U(t) = \exp[i\vec{\sigma}\cdot\vec{\varphi}(t)]$ with $\vec{\sigma} = (\sigma_x, \sigma_y, \sigma_z)$, $\vec{\varphi}(t) = (\varphi(t)/\sin[\varphi(t)])(\Sigma_{m=0}^{\infty} R_x^{(2m+1)}(t), \Sigma_{m=0}^{\infty} R_y^{(2m+1)}(t), \Sigma_{m=0}^{\infty} R_y^{(2m)}(t))$, and $\varphi(t) = \cos^{-1}(\Sigma_{m=0}^{\infty} R_x^{(2m)}(t))$. Here

$$R_x^m(t) = (-1)^{[(m+1)/2]}\left(\prod_{l=1}^{m}\int_0^t dt_l\right)\theta(t_1 - t_2)\cdots\theta(t_{m-1} - t_m)X_m,$$

$$R_y^m(t) = (-1)^{[(m+1)/2]}\left(\prod_{l=1}^{m}\int_0^t dt_l\right)\theta(t_1 - t_2)\cdots\theta(t_{m-1} - t_m)Y_m,$$

$$X_m = (Z_m + Z_m^*)/2, \quad Y_m = (-1)^m(Z_m - Z_m^*)/2i,$$

and

$$Z_m = \prod_{l=1}^{m}\phi(t_l)e^{i(-1)^l\Delta t_l}.$$

The formula may look complex, yet some interesting features can be found from it. The above expansion has an interpretation in terms of Feynman diagrams. Each interaction vortex associated with a factor $e^{i(-1)^l\Delta t_l}g\cos(k+\nu t_l)$ [or $e^{i(-1)^l\Delta t_l}G\cos(\omega_0 t_l)$] corresponds to the process of absorption/emission a $E$-photon ($D$-photon) and the electron moving from state $|i\rangle$ to $|j\rangle$, $i,j = 1,2$. In the THz regime, which we are mainly interested in, the largest energy scale is $\Delta \gg \hbar\omega_o$, $\hbar\nu$. Thus in a physical process, whenever there is a energy change $\Delta$ at one interaction vortex, there must be another energy change $-\Delta$ at another interaction vortex due to energy conservation. Therefore there is a conservation law $n+m$=even number for the process with $m$ $E$ photons and $n$ $D$ photons involved. Since $g$ is usually very small, the weight

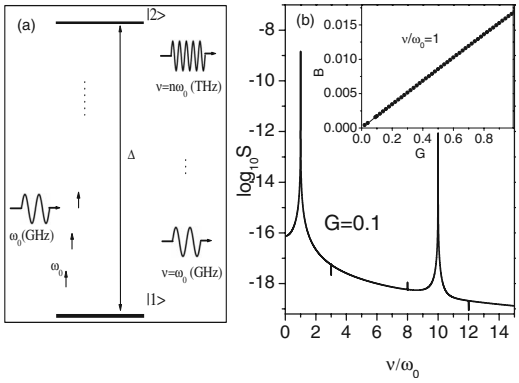


FIG. 1. (a) Schematic representation of our system and related optical processes; (b) emission spectrum for weak driving field $G=0.1$. Insert: Quasienergy bandwidth versus $G$ for $\nu=1$ in the weak driving regime.

for each process with $n$ $D$ photons involved is $gG^n$. For weak driving field, the number of excited $D$ photon is small and only one $D$-photon process is important, thus there is a resonance at $\nu=\omega_0$. While for strong driving situation $G \gg 1$, multi-$D$-photon process becomes also important, then there are resonant peaks at $\nu=n\omega_0$, $n$ odd number due to the conservation law $1+n$=even number.

More qualitative understanding of THz generation can be obtained through the picture of particle transport in two chains. Basically, the further the particle propagates, the more photons are generated in the dual picture. Here the Floquet theorem[8] for a system driven by time-periodic field is important and the quasienergy spectrum may play an essential role. The wider the quasienergy bandwidth is, the faster the particle moves away, the more photons are generated. To get more understanding of the system with confined electrons, $D$ photons, and $E$ photons involved and make a further step in the analytical calculation, we perform a perturbative calculation. The quasienergy spectrum can be calculated by diagonalizing the time evolution operator $U(T=2\pi/\omega_0)$. Since the electron-$E$-photon interaction is weak, and to the first order of electron-$D$-photon interaction, we have

$$\varepsilon_{\pm}(k) \propto \pm[C + gG\sin(k)], \quad (4)$$

with $C$ a constant for $\nu=1$, $\Delta \gg \hbar\omega$, $\hbar\nu$.

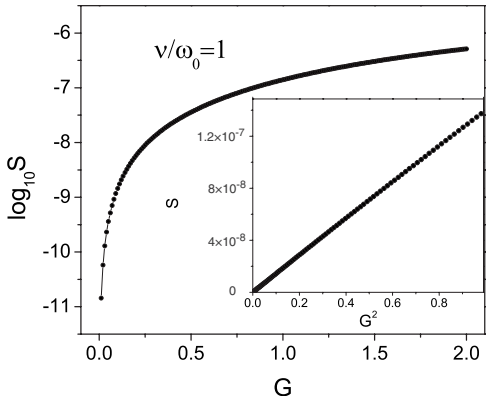


FIG. 2. Emission intensity versus $G$ for $\nu=1$. Main panel: $\mathrm{Log}_{10}\,S$ versus $G$; Insert: $S$ versus $G^2$.

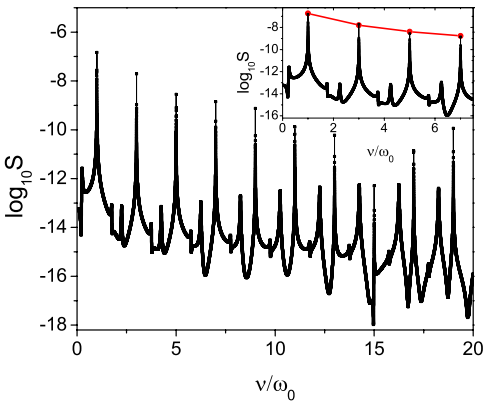


FIG. 3. (Color online) Emission spectrum for strong driving field $G=30$. Insert: the red line is for that from $\log_{10}(C_1B^2/\nu)$, $\nu=1,3,5,7$, where $B$ is the bandwidth from Fig. 4 and $C_1$ is a constant.

### III. NUMERICAL RESULTS AND DISCUSSIONS

We numerically calculate the quasienergy spectrum by exact diagonalizing the time evolution operator $U(T)$. $U(T)$ is obtained by numerical integration $U(T)=\hat{T}\int_0^T \exp\{iH_{eff}(t)dt\}$, with initial condition $U(t=0)=I$, time step $2\pi/5000$ and $\hat{T}$ referring to time order. We have used evolution operator matrix of size $50\times 50$ in the basis of $|i,n_i\rangle$, $i=1,2$ for diagonalization. The emission spectrum can also be obtained conveniently by the Fourier transformation of the dipole moment,[13] which is solved by the Runge-Kutta method with time step of 0.01 and total time of 16000. We have used the driving field frequency $\hbar\omega_0$ ($\omega_0=100$ GHz) as the unit of energy and $g=0.005$, $\Delta=10$.

Figure 1(b) shows the emission spectrum for weak driving field. Two resonant peaks at $\nu=\omega_0$ and $\nu=\Delta$ are clearly seen. Clearer physical picture can be obtained by looking at the quasienergy spectrum. As one can see in the insert of Fig. 1(b), the bandwidth of the quasienergy band is proportional to $G$ for small $G$, which is consistent with Eq. (4). The emission intensity versus $G$ is displayed in Fig. 2. There it is seen that the emission intensity increases as $G$ increases. Moreover, the emission intensity $S\sim G^2$ as seen in the insert. Basically, in the weak driving regime, the emission intensity $S$ is proportional to the probability for electron in the excited state, which is proportional to $G^2$. Combining with the fact that $B\propto G$ [Eq. (4) and Fig. 1(b)], we have $S\propto B^2$.

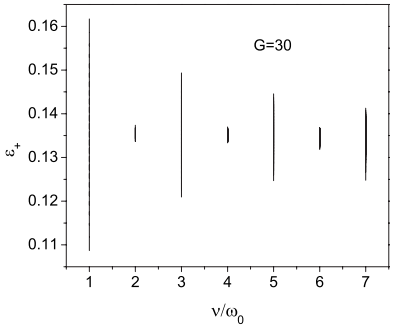


FIG. 4. Quasienergy versus integer $\nu/\omega_0$. $G=30$.

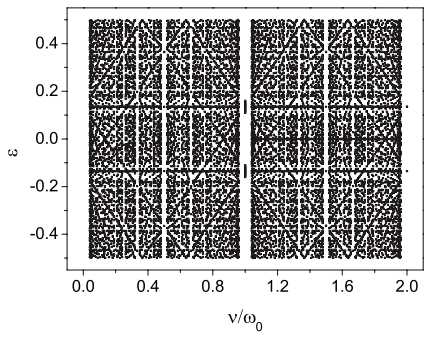


FIG. 5. Quasienergy versus fractional $\nu/\omega_0$. $G=30$.

Let's look at a more interesting situation with strong driving field. The emission spectrum is shown in Fig. 3. It is quite different from that in the weak driving regime. Here we see a series of peaks at odd $E$-photon frequencies (in units of $D$-photon frequency), which is due to the conservation law discussed before. The quasienergy spectra for integer photon frequency and fractional photon frequency are shown in Figs. 4 and 5. It is obvious that the quasienergy bandwidth for odd frequency is much wider than those for even frequency. The quasienergy spectrum for fractional frequency is discrete point spectrum and shows interesting fractal structure (similar fractal spectrum was observed in other systems[7,14]). The similarity between the fractal quasienergy and Hofstadter's butterfly-energy spectrum[15] of a Bloch electron in a two-dimensional lattice in the presence of a constant magnetic field is due to the congruence between electric and magnetic problems (with $\hbar\nu_q$ mapped to the spacing of Wannier-Stark ladders in the charge transport picture).[14] The quasienergy spectrum gives the information of the emission spectrum in Fig. 3. From the dual picture of particle transport, the wider the bandwidth is, the faster the particle moves to larger lattice site, which corresponds to more photons being emitted. Moreover the quasienergy bandwidth completely determines the emission intensity for fixed $G$. As seen in the insert of Fig. 3, the formula $S\propto B^2/\nu$ fits well with the emission spectrum for $\nu=1,3,5,7$ with $B$ obtained from exact numerical calculation. In principle, $S\propto B^2/\nu$ can also give the values of emission intensity for other values of $\nu$. Yet, the bandwidth for other $\nu$ is too small to be obtained within current accuracy.

Here we have seen that the picture of particle transport helps us to understand the photon emission. One interesting phenomenon in particle transport driven by time-periodic

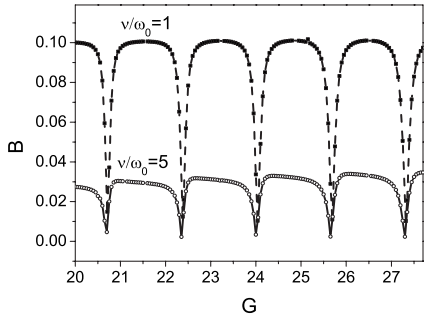


FIG. 6. Quasienergy bandwidth versus $G$ for $\nu=1,5$.

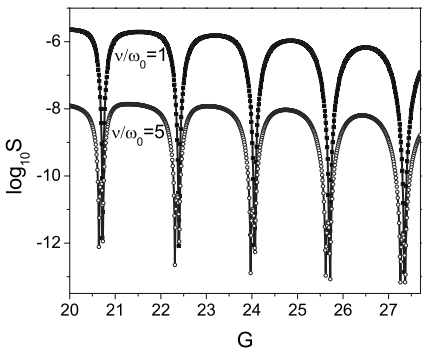


FIG. 7. Emission intensity versus $G$ for $\nu=1,5$.

field is the field induced localization.[9] That is, under suitable conditions when the band collapse (i.e., the bandwidth becomes zero)[10] happens, the effective mass of the particle becomes infinity and it localizes due to coherent destruction of tunneling (CDT).[11] It's interesting to see the corresponding phenomenon in the optical processes. Figure 6 shows the quasienergy bandwidth versus G. We see that at some specific points $G=20.7,22.4,24.0...$, the bandwidth is very small, i.e., band collapse happens. Under the conditions of band collapse, the full emission spectrum is suppressed for the parameters we used. The photon emission intensities for $\nu/\omega_0=1,5$ are shown in Fig. 7, where one sees that there are a series of dips exactly at the positions corresponding to band collapse. The ratio of the maximum emission intensity to the minimum emission intensity is around $10^6$.

From the above results, we find that it is not always good to increase the driving field to generate strong THz radiation. The quasienergy spectrum can give the optimal conditions (corresponding to resonant conditions) and dynamic quench conditions (corresponding to band collapses/CDT) for photon emission.

Basically, our approach suggests a way to generate THz radiation through semiconductor quantum dots driven by GHz waves, which can be obtained by various ways such as IMPATT diode. One advantage of this method is that high quantity low-frequency sources are easier to obtain. For instance, the power density of IMPATT diode at 10–100 GHz could reach 10 $\mathrm{KW/cm^2}$.[16] In this way, we may obtain THz radiation with appreciable power of the order $\mu$W (under appropriate conditions) at frequency $20\times\nu=0.2-2$ THz, which is usually the most difficult regime for THz wave generation. Another advantage of our method is that the THz wave obtained is multiple modes (with different frequencies), unlike that from QCL.

## IV. SUMMARY

We have proposed to generate THz (0.2–2 THz) radiation through high-order harmonic fields in semiconductor quantum dots driven by GHz (10–100 GHz) waves. By mapping the optical problem of generating THz radiation to an equivalent particle transport problem, we have found a relation between the quasienergy spectrum and emission intensity. The optimal conditions (corresponding to resonant conditions) and dynamic quench conditions (corresponding to band collapses/CDT) for photon emission are found. The very nice on/off properties (the ratio of intensity at resonance to that at quench condition $\sim 10^6$) should have important applications. Our studies are also useful for the devices working with THz wave.

## ACKNOWLEDGMENTS

This work was partially supported by the National Science Foundation of China under Grants No. 10574017, No. 10744004, No. 10774016, and No. 10874020, National Fundamental Research of China under Grant No. 2006CB921400, and a grant of the China Academy of Engineering and Physics.

*Author to whom correspondence should be addressed. zhang_wei@iapcm.ac.cn

[1] M. Tonouchi, Nat. Photonics **1**, 97 (2007).
[2] M. A. Belkin, F. Capasso, A. Belyanin, D. L. Sivco, A. Y. Cho, D. C. Oakley, C. J. Vineis, and G. W. Turner, Nat. Photonics **1**, 288 (2007).
[3] G. Ramian, Nucl. Instrum. Methods Phys. Res. A **318**, 225 (1992).
[4] R. Kohler, A. Tredicucci, F. Beltram, H. E. Beere, E. H. Linfield, A. G. Davies, D. A. Ritchie, R. C. Iotti, and F. Rossi, Nature (London) **417**, 156 (2002); B. S. Williams, Nat. Photonics **1**, 517 (2007).
[5] K. J. Ahn, F. Milde, and A. Knorr, Phys. Rev. Lett. **98**, 027401 (2007).
[6] Y. Chassagneux, Nature (London) **457**, 174 (2009).
[7] W. Zhang and X.-G. Zhao, Physica B **291**, 299 (2000); D. Suqing, W. Zhang, and X.-G. Zhao, Phys. Rev. B **62**, 9943 (2000); D. Suqing, W. Zhang, and X.-G. Zhao, Physica E **9**, 659 (2001).
[8] J. H. Shirley, Phys. Rev. **138**, B979 (1965).
[9] D. H. Dunlap and V. M. Kenkre, Phys. Rev. B **34**, 3625 (1986); X.-G. Zhao, Phys. Lett. A **155**, 299 (1991); **167**, 291 (1992); B. J. Keay, S. Zeuner, S. J. Allen, Jr., K. D. Maranowski, A. C. Gossard, U. Bhattacharya, and M. J. W. Rodwell, Phys. Rev. Lett. **75**, 4102 (1995); S. Longhi, M. Marangoni, M. Lobino, R. Ramponi, P. Laporta, E. Cianci, and V. Foglietti, *ibid.* **96**, 243901 (2006); R. Iyer, J. S. Aitchison, J. Wan, M. M. Dignam, and C. M. de Sterke, Opt. Express **15**, 3212 (2007).
[10] M. Holthaus, Phys. Rev. Lett. **69**, 351 (1992).
[11] F. Grossmann, T. Dittrich, P. Jung, and P. Hänggi, Phys. Rev. Lett. **67**, 516 (1991).
[12] X.-G. Zhao, Phys. Lett. A **193**, 5 (1994).
[13] C. Liu, S. Gong, R. Li, and Z. Xu, Phys. Rev. A **69**, 023406 (2004).
[14] X.-G. Zhao, R. Jahnke, and Q. Niu, Phys. Lett. A **202**, 297 (1995); X-G. Zhao and Q. Niu, *ibid.* **191**, 181 (1994).
[15] D. R. Hofstadter, Phys. Rev. B **14**, 2239 (1976).
[16] R. De La Cruz and A. Zemliak, *Characteristics of the Double Avalanche Region IMPATT Diode in Millimetric Range*, 14th International Conference on Electronics, Communications and Computers (IEEE Computer Society, Washington, DC, 2004), p. 223.